BIOCHEMISTRY
including biophysical chemistry & molecular biology

Article

pubs.acs.org/biochemistry

Mechanism of Inhibition of Fatty Acid Amide Hydrolase by Sulfonamide-Containing Benzothiazoles: Long Residence Time Derived from Increased Kinetic Barrier and Not Exclusively from Thermodynamic Potency

Gaochao Tian,*[,†,#] Kathy A. Paschetto,[†] Farzin Gharahdaghi,[∥] Euan Gordon,[⊥] Dee E. Wilkins,[†,&] Xincai Luo,[‡] and Clay W. Scott[§]

[†]Lead Generation, [‡]Chemistry, and [§]Molecular and Investigative Toxicology, AstraZeneca Pharmaceuticals, 1800 Concord Pike, Wilmington, Delaware 19850, United States

[∥]Bioscience, Oncology, AstraZeneca Pharmaceuticals, 35 Gatehouse Drive, Waltham, Massachusetts 02451, United States

[⊥]Innovative Medicines, DECS, AstraZeneca Pharmaceuticals, Pepparedsleden 1, 43183 Mölndal, Sweden

ABSTRACT: Fatty acid amide hydrolase (FAAH) has emerged as a potential target for developing analgesic, anxiolytic, antidepressant, sleep-enhancing, and anti-inflammatory drugs, and tremendous efforts have been made to discover potent and selective inhibitors of FAAH. Most known potent FAAH inhibitors described to date employ covalent mechanisms, inhibiting the enzyme either reversibly or irreversibly. Recently, a benzothiazole-based analogue (**1**) has been described possessing a high potency against FAAH yet lacking a structural feature previously known to interact with FAAH covalently. However, covalent inhibition of FAAH by **1** has not been fully ruled out, and the issue of reversibility has not been addressed. Confirming previous reports, **1** inhibited recombinant human FAAH (rhFAAH) with high potency with IC_{50} ~2 nM. It displayed an apparently noncompetitive and irreversible inhibition, titrating rhFAAH stoichiometrically within normal assay times. The inhibition appeared to be time dependent, but the time dependence only improved potency by a small degree (from ~8 to ~2 nM). However, mass spectrometric analyses of the reaction mixture failed to reveal any cleavage product or covalent adduct and showed full recovery of the parent compound, ruling out covalent, irreversible inhibition. Dialysis revealed recovery of enzyme activity from enzyme−inhibitor complex over a prolonged time (>10 h), demonstrating that **1** is indeed a reversible, albeit slowly dissociating inhibitor of FAAH. Molecular docking indicated that the sulfonamide group of **1** could form hydrogen bonds with several residues involved in catalysis, thereby mimicking the transition state. The long residence time displayed by **1** does not appear to derive exclusively from great thermodynamic potency and is consistent with an increased kinetic energy barrier that prevents dissociation from happening quickly.

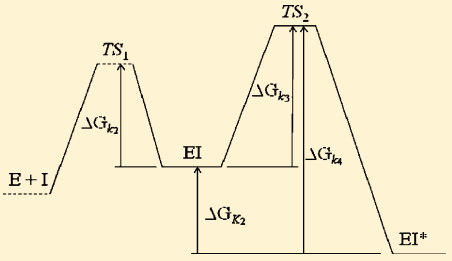

Fatty acid amide hydrolase (FAAH)[1] is a member of the amidase signature serine hydrolases[2] and catalyzes degradation of several fatty acid amide lipid transmitters that are implicated in behavioral and physiological conditions.[3] For example, anandamide, a cannabinoid receptor 1 (CB1) specific agonist,[4] has been shown to regulate pain, mobility, cognition, and feeding.[3] Genetic knockout[5] or biochemical inhibition of FAAH[6] leads to greatly elevated endogenous levels of these fatty acid amides throughout the nervous system with concomitant analgesic,[7−11] antidepressant,[12,13] anxiolytic,[6] sleep-enhancing,[14] memory-acquiring,[15] and anti-inflammatory[7,16−19] phenotypes. Notably, these phenotypes occur in the absence of any defects in motility, weight, or body temperature that are commonly associated with direct application of CB1 agonists,[5−7,9−12,18] suggesting that FAAH inhibition may be a more attractive strategy than direct CB1 agonism.

A variety of structurally diverse FAAH inhibitors have been described,[3,20,21] inhibiting the enzyme by either covalent or noncovalent mechanisms. Covalent inhibitors dominate the field and their mechanisms of inhibition are well characterized, as exemplified by the studies on fluorosulfonates,[22,23] fluorophosphonates,[24−26] trifluoromethyl ketones,[27−29] α-keto heterocycles,[30−32] carbamates,[33−37] and arylureas.[38−41] While trifluoromethyl ketones and α-keto heterocycles form reversible hemiacetal transition state mimetics, fluorosulfonates, fluorophosphonates, carbamates, and arylureas modify the catalytic serine and therefore are mechanism-based, irreversible inhibitors. Mainly due to their covalent interaction with the enzyme,[28] these inhibitors display superb potency *in vitro*, and some, including α-keto heterocycles,[21] carbamates,[6,9,11−13,18] and arylureas,[41] show efficacy *in vivo*.

Although covalent inhibitors have shown promise in preclinical models, it remains desirable to identify potent inhibitors that only utilize noncovalent interactions rather than employ chemical reactivity, which could in principle lead to potential off-target liabilities. Early known noncovalent inhibitors of FAAH, such as NSAIDs[42,43] and substrate analogues,[44−46] are far weaker in potency than covalent inhibitors, limiting their

Received: April 12, 2011
Revised: June 29, 2011
Published: July 5, 2011

ACS Publications © 2011 American Chemical Society

application *in vivo*. Recently, a number of pharmaceutical research institutes have carried out high-throughput screens against FAAH, but the full scope of these efforts has yet to be described. Given the lack of structural information on FAAH complexed with any noncovalent inhibitors, the detailed mechanism of interaction and therefore how these inhibitors derive their potency remains poorly understood.

In the current investigation, we conducted kinetic and mass spectrometric studies on a sulfonamide-containing benzothiazole-based analogue, **1**, which has been described recently as a potent, low nM FAAH inhibitor.[47] This novel FAAH inhibitor does not possess a covalent "warhead" of known irreversible FAAH inhibitors, such as fluorophosphonate, α-ketone heterocycle, carbamate, or arylurea, but contains intriguing structural features of both an amide and sulfonamide. Although its inhibition of FAAH does not appear to be time-dependent as reported by Wang et al.,[47] covalent interaction with FAAH has not been fully ruled out, and the issue of reversibility has not been addressed. Data from the current study demonstrated that **1** is potent, but indeed noncovalent and reversible, albeit slowly dissociating, resulting in the inhibitor displaying a long residence time ($t_{1/2}$ > 10 h). Detailed analysis of the kinetics and energetics of the inhibition revealed a two-step, time-dependent inhibition mechanism with an increased kinetic barrier, rather than an exclusive, great thermodynamic potency, as the main reason for the observed long inhibitor residence time.

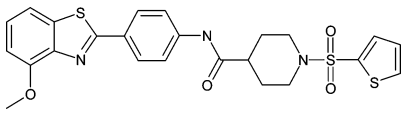

1

EXPERIMENTAL PROCEDURES

Materials. Tris-HCl, BSA, EDTA, and DMSO were purchased from Sigma. Anandamide [ethanolamine 1-^{3}H] was purchased from American Radiolabeled Chemicals. Black 384-well OptiPlates were purchased from Perkin-Elmer. Slide-A-Lyzer dialysis cassettes were purchased from Pierce. The benzothiazole analogue **1** (*N*-(4-(6-methylbenzo[*d*]thiazol-2-yl)phenyl)-1-(thiophen-2-ylsulfonyl)piperidine-4-carboxamide) and D-AMC were synthesized at AstraZeneca Pharmaceuticals in Wilmington, DE.

Preparation of Recombinant Human FAAH Membranes. CHO cells adapted to grow in suspension (Life Technology) were transfected through electroporation with pLINAZ-hFAAH, which was prepared by subcloning of the human FAAH cDNA (Origene) into a pLINAZ vector. A CHO clone with high, stable expression of FAAH activity was chosen for expansion. Freshly collected cells or frozen cell pellets stably expressing recombinant human FAAH (rhFAAH) were suspended in ice-cold buffer (50 mM HEPES, pH 8, containing 1 mM EDTA, 1 mM pepstatin, 100 mM leupeptin, and 0.1 mg/mL aprotinin) and homogenized with a Polytron. The cell fragments were centrifuged at 1000*g*, discarding the pellet. The saved supernatant was centrifuged at 150000*g* to pellet the remaining membranes. That pellet was diluted to 35 mg/mL, aliquoted, snap-frozen in liquid nitrogen, and stored at −80 °C.

Preparation of Humanized Rat FAAH. Humanized rat FAAH (h/FAAH) was expressed and purified according to procedures described previously.[48]

Inhibition Assays of rhFAAH. The enzyme activity of rhFAAH was measured according to published procedures with minor modifications by either a fluorescent assay using D-AMC[50] or a radioactive assay using tritium-labeled anandamide (^{3}H-anandamide)[51] as substrate. The assay buffer was 150 mM Tris-HCl, pH 8.0, containing 0.5 mM EDTA and 1 mg/mL BSA, and these conditions were used throughout the entire investigation unless specified otherwise. In the fluorescent assay, 1 μL of DMSO (as control) or inhibitor at a specified concentration in DMSO was spotted at the bottom of a well of a black 384-well OptiPlate. Assay buffer (9 μL) containing a final concentration of 35 μg/mL rhFAAH membranes was added, and the mixture was incubated for 45 min. Assay buffer (20 μL) containing D-AMC at a final concentration of 1 μM was added to initiate assay. Incubated at room temperature (22 °C) for 4 h, the plate was read on an Envision to measure fluorescent signal in each well. In the radioactive ^{3}H-anadamide assay, 50 μL of rhFAAH membranes at a concentration of 1 μg/mL was mixed with 10 μL of buffer and 40 μL of 25 nM (or specified otherwise) anandamide [ethanolamine 1-^{3}H] in a 96-well polypropylene plate. The assay plate was incubated at room temperature for 30 min. The assay mixture (60 μL) was then transferred onto prewetted charcoal minicolumns that had been prepared in a 96-well Millipore filter plate. The charcoal-containing filter plate was stacked on top of a Perkin-Elmer Picoplate and centrifuged at 500*g* for 4 min to remove unreacted anandamide [ethanolamine 1-^{3}H], with the eluate containing ^{3}H-ethanolamine captured in the Picoplate. Assay buffer (50 μL) without BSA was added to each minicolumn of the charcoal-containing filter plate, and the plate stack was centrifuged again. Finally, 200 μL of Microscint-40 was added to the eluate in the Picoplate, and the plate was read in a TopCount scintillation counter.

Inhibitor Reversibility Assays. Reversibility of inhibition was assessed by two different procedures. The first was a centrifugation and wash procedure. In this procedure, 8 μL of enzyme at 35 μg/mL (final concentration) and 2 μL of inhibitor at a specified concentration were incubated in assay buffer at 22 °C for 45 min. The mixture was then diluted 1:100 by adding 990 μL of assay buffer, and this 1 mL initial dilution mixture was centrifuged at 48000 rpm (100000*g*) for 30 min. The supernatant was discarded, and the pellet was resuspended in 1 mL of assay buffer. The suspension was centrifuged again at 48000 rpm for 30 min. The pellet was resuspended in 1 mL of 1 μM D-AMC in assay buffer at 22 °C. Aliquots were transferred to a black 384-well OptiPlate to read on Envision after 4 h. In the second procedure, the initial 1 mL dilution mixture of enzyme−inhibitor complex was prepared in the same way as in the first procedure, but instead of being put through the centrifugation and wash procedure, it was placed in a Slide-A-Lyzer dialysis cassette with a molecular weight cutoff of 10000. This dialysis cassette was placed in 4 L of assay buffer that had been pre-equilibrated at 4 °C. An aliquot was withdrawn using a syringe at different times over a period of 18 h to determine FAAH activity using the D-AMC assay.

Liquid Chromatography Electrospray Mass Spectrometric Assays. To determine product formation and quantify compound recovery, 2 μL of rhFAAH membranes or CHO cell membranes (17.5 mg/mL) and 1 μL of inhibitor at a specified concentration were mixed in 7 μL assay buffer, and the mixture was incubated at 22 °C for 18 h. The mixture was diluted in 90 μL of acetonitrile, desalted by reverse phase liquid chromatography (Agilent 1200 Series Rapid Resolution LC

System), and then injected into an electrospray ionization mass spectrometry (ESI-MS) apparatus (Agilent 6410 triple quadrupole). Product formation was determined by isolating and identifying fragments of target ions through multiple LC/MS/MS experiments. Compound recovery was quantified using a standard concentration curve ($r^2 > 0.99$) with measurements made based on peak areas.

To determine covalent adduct formation, 30 μg of recombinant h/rFAAH protein was incubated with 80 μM inhibitor at room temperature for 1 h in 60 μL of 10 mM HEPES, pH 8.0, containing 100 mM NaCl and 0.002% DDM. The sample (50 μL) was desalted by reverse phase chromatography (gradient: 95−0% acetonitrile in water containing 0.5% trifluoroacetic acid) before injection into an ESI-MS apparatus (MassLynx (Waters)) in positive ion (ES+) mode. Peak masses were determined by the MaxEnt Deconvolution software (Waters).

Computer-Modeling of Interactions of the Benzothiazole Analogue 1 with h/rFAAH by Induced Fit Docking. An induced fit docking exercise was performed using a procedure based on the Glide 5.0 docking program and the Prime 1.7 protein structure prediction and refinement program from Schrodinger. The 3D coordinates of the h/rFAAH structure[48] for this study were taken from RCSBProtein Data Bank (PDB code: 2VYA). The protein structure was treated with a standard protein preparation procedure using the Schrödinger Protein Preparation Wizard to assign proper bond orders and add hydrogen atoms to heavy atoms in the PDB file. The benzothiazole analogue **1** was docked into the binding pocket of h/rFAAH with Glide 5.0, and the top 20 poses were refined with Prime 1.7 for all the residues located 5 Å from the ligand. This was followed by redocking **1** into the refined protein structures, maintaining only the pose with the best docking score.

Data Analysis. IC_{50} values from inhibition kinetics were determined by subtracting background from total signal (fluorescent or radioactive), determining the percentage of activity (%Act) relative to the maximum values measured in the absence of inhibitor I, and then fitting %Act as a function of inhibitor concentration according to eq 1:

$$\%\mathrm{Act} = 100\left(1 - \frac{[\mathrm{I}]}{\mathrm{IC}_{50} + [\mathrm{I}]}\right) \quad (1)$$

Time-dependent inhibition may be described by the following kinetic mechanism (eq 2):

$$\mathrm{E} + \mathrm{I} \overset{K_i}{\rightleftharpoons} \mathrm{EI} \underset{k_4}{\overset{k_3}{\rightleftharpoons}} \mathrm{EI}^* \quad (2)$$

where K_i is the inhibition constant for the binding of inhibitor and enzyme (E) to form an initial enzyme−inhibitor complex (EI) and k_3 and k_4 are the forward and reverse rate constants, respectively, of the subsequent time-dependent isomerization that leads to the formation of the enzyme−inhibitor complex (EI*). Progress curves in an enzyme reaction in the presence of a time-dependent inhibitor can be then described according to eq 3:

$$P = \upsilon_s t + \frac{\upsilon_i - \upsilon_s}{k_{obsd}}(1 - e^{-k_{obsd}t}) \quad (3)$$

where P is product, υ_i is enzyme initial velocity at $t = 0$, υ_s is enzyme initial velocity at steady state, and k_{obsd} is the observed rate constant for inhibition. Progress curves analyses were performed to provide estimates of k_{obsd} and υ_i. Further analysis of k_{obsd} according to eq 4 provided estimates of K_i for the initial binding step and the rate constants k_3 and k_4:

$$k_{obsd} = \frac{k_3[\mathrm{I}]}{K_i + [\mathrm{I}]} + k_4 \quad (4)$$

assuming $[S] \ll K_m$. K_i was also estimated by analyzing υ_i according to eq 5:

$$\%\upsilon_{i([I]=0)} = 100\left(1 - \frac{[\mathrm{I}]}{K_i + [\mathrm{I}]}\right) \quad (5)$$

where $\upsilon_{i([I]=0)}$ is initial velocity at $[I] = 0$.

RESULTS

Benzothiazole Analogue 1 Is a Potent, Low nM Inhibitor of rhFAAH. A number of FAAH assays had been described in the literature, including a fluorescence assay using decanoyl 7-amino-4-methylcoumarin (D-AMC) as substrate[50] and a radioactive assay using ^{3}H-anandamide as substrate.[51] In the D-AMC assay, cleavage of substrate releases the 7-amino-4-methylcoumarin (AMC) moiety, allowing measurements of FAAH activity by monitoring fluorescence derived from AMC. In the ^{3}H-anandamide assay, the FAAH reaction produces [^{3}H]ethanolamine, which is then quantified by measuring radioactivity after separating [^{3}H]ethanolamine from ^{3}H-anandamide by filtering the assay mixture through charcoal. Both these assays were used to determine the potency of **1** for the inhibition of rhFAAH. In the ^{3}H-anandamide assay, **1** gave an IC_{50} of 2.0 ± 0.4 nM (Figure 1). Consistent with this data, **1** displayed an IC_{50} of 2.6 ± 0.6 nM in the fluorescent D-AMC assay (Figure 1). These data confirmed the high potency (1.7 nM) of **1** as reported previously.[47]

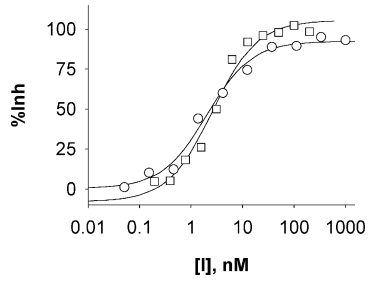

Figure 1. Plots of percent inhibition (%Inh) of rhFAAH against the concentration of benzothiazole analogue **1**. Potency of the benzothiazole analogue **1** was assessed at pH 8.0 and 22 °C with a radioactive assay using ^{3}H-anandamide (○) and a fluorescent assay using D-AMC (□).

Benzothiazole Analogue 1 Appears To Inhibit rhFAAH Noncompetitively. To determine the mode of inhibition of rhFAAH by **1**, inhibitor concentration−response curves were determined at several ^{3}H-anandamide concentrations both below and above the K_m (1.4 ± 0.3 μM, unpublished data). Increased concentrations of substrate did not seem to appreciably reduce the potency of **1** (Figure 2). As listed in Table 1, the IC_{50} for **1** increased less than 3-fold over the substrate concentration range of 0.078−10 μM (concentrations greater than 10 μM were not used in this experiment as

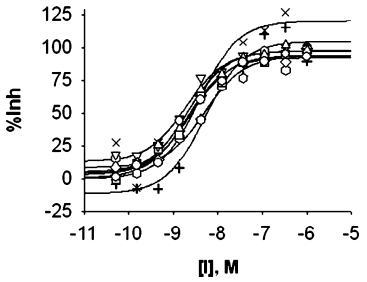

Figure 2. Plots of percent inhibition (%Inh) of rhFAAH against the concentration of benzothiazole analogue **1** at various concentrations of anandamide. Potency of the benzothiazole analogue **1** was assessed at pH 8.0 and 22 °C with a radioactive assay using ^{3}H-anandamide at 0.078 (○), 0.16 (△), 0.31 (▽), 0.63 (□), 1.3 (◇), 2.5 (⬡), 5.0 (+), and 10 μM (×) concentrations.

Table 1. Summary of IC_{50} Values for Benzothiazole Analogue 1 at Different Substrate Concentrations[a]

[^{3}H-anandamide], μM	IC_{50}, nM	[^{3}H-anandamide], μM	IC_{50}, nM
0.078	2.0 ± 0.4	1.3	2.5 ± 0.4
0.16	2.1 ± 0.3	2.5	5.1 ± 1.6
0.31	2.0 ± 0.4	5.0	5.1 ± 1.7
0.63	2.3 ± 0.4	10	3.8 ± 2.1

[a]The values were obtained through least-squares analysis (eq 1) of concentration-response data produced using the ^{3}H-anandamide assay at pH 8.0 and 22 °C.

substrate inhibition started to take place beyond this substrate concentration, unpublished observation), indicating that inhibition of rhFAAH by **1** under these conditions could not be strictly competitive. Usually noncompetitive inhibition derives from binding of inhibitor at a pocket separate from active site. However, nonequilibrium conditions, such as irreversible inhibition, can lead to an apparent noncompetitive inhibition pattern despite binding of inhibitor at the active site. The second possibility warranted additional tests given the precedents of covalent irreversible inhibitors for this enzyme and theoretical potential of amides or sulfonamides to act by covalent mechanisms.

Preincubation and Dilution Fails To Recover rhFAAH Activity. A commonly used approach to assessing reversibility of inhibition is a preincubation and dilution procedure, where enzyme is preincubated with inhibitor to form the enzyme–inhibitor complex and then diluted into an assay solution, reducing inhibitor concentration below its IC_{50}. If enzyme activity recovers after dilution, the inhibition must be reversible. If it does not, the result suggests, but does not prove, irreversibility. Membranes of rhFAAH were preincubated for 45 min with 1 μM of **1**, conditions that would result in formation of a fully occupied enzyme–inhibitor complex. The preincubation mixture was then subjected to a wash and centrifugation protocol leading to a total 1000000-fold dilution of inhibitor or a final inhibitor concentration of 0.001 nM, a value ~2000-fold less than the IC_{50} for **1**. The same procedure was performed with two well-documented potent reference compounds URB597, a carbamate inhibiting FAAH covalently and irreversibly,[35] and OL-135, an α-keto-heterocycle that is a covalent reversible inhibitor of FAAH.[30] As shown in Figure 3, FAAH activity did not recover from preincubation and dilution with URB597, whereas it fully recovered from the same experiment with OL-135, results consistent with the known

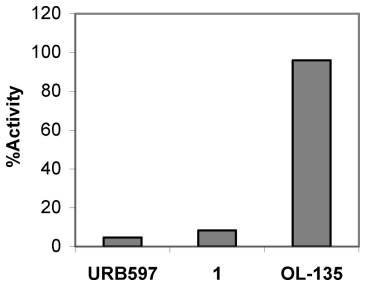

Figure 3. Recovery of rhFAAH activity after incubation with inhibitors. Membranes of rhFAAH at 35 μg/mL (final concentration) were incubated with 1 μM inhibitor at pH 8.0 at 22 °C for 45 min. The mixture was then diluted and centrifuged to remove excess inhibitor. The pellet was resuspended and measured for enzyme activity using the D-AMC assay. The activities recovered were plotted as percent of control where enzyme was incubated in the absence of inhibitor.

mechanistic properties of these inhibitors. The benzothiazole analogue **1** behaved similarly to URB597 in this procedure, increasing our suspicion that this inhibitor might be no different from many other potent FAAH inhibitors, interacting with the enzyme covalently and inhibiting FAAH irreversibly.

Benzothiazole Analogue 1 Titrates rhFAAH. To rule out traces of chemically reactive contaminants in **1** as the reason for the observed failure to recover FAAH activity using preincubation and dilution as described above, enzyme titration kinetics was carried out. In this procedure, enzyme at varying concentrations is incubated with inhibitor at a fixed concentration. Plotting enzyme activity as a function of enzyme concentration reveals a turning point, which corresponds to the concentration of enzyme inhibited by an equimolar concentration of the test compound (assuming stoichiometric formation of an enzyme–inhibitor complex). Since the rhFAAH used in the mechanistic investigation was not purified and the actual enzyme concentration in the membrane preparation was unknown, the enzyme titration kinetics were run with **1** as well as the irreversible inhibitor URB597 as a control. If the inhibition by **1** is due to a minor contaminant, this sample would show a turning point at a much lower membrane concentration compared to URB597. If inhibition is not due to a contaminant, then **1** and URB597 would show turning points at the same membrane concentration, and this would represent the amount of membrane preparation that contained the same molar concentration of rhFAAH enzyme as inhibitor. As shown in Figure 4, 25 nM **1** and URB597 produced very similar titration plots with turning points at a virtually identical membrane concentration (258 and 268 μg/mL, respectively). These results strongly argue against the possibility of trace amount of chemically reactive contaminants present in **1** as the reason for the observed failure of FAAH activity to recover by the preincubation and dilution procedure.

The enzyme titration data described above also revealed that 1 μg/mL membrane preparation contained about 0.1 nM rhFAAH. Since the final membrane protein concentration used in the fluorescent D-AMC assay was 35 μg/mL, the molar enzyme concentration used in the inhibition studies would be calculated to be about 3.5 nM according to this enzyme titration data. This raised the possibility that the actual potency of compound **1** might have been underestimated by using this

dx.doi.org/10.1021/bi200552p | Biochemistry 2011, 50, 6867–6878

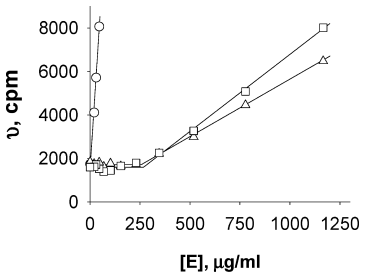

Figure 4. Titration of rhFAAH by the benzothiazole analogue **1** and URB597. Membranes of rhFAAH at different concentrations were incubated at pH 8.0 and 22 °C for 1 h in the absence of inhibitor (○) or with 25 nM **1** (△) or URB597 (□). The enzyme activities were determined by measuring initial rates (v), which were then plotted against enzyme concentration. In the absence of inhibitor, the plot was linear, whereas in the presence of inhibitor the initial rates were flat for enzyme concentrations up to 258 and 268 μg/mL respectively for **1** and URB597 and became linear with higher enzyme concentrations. The enzyme concentrations at these turning points are equivalent to the concentration of inhibitor in the preincubation mixture, thereby providing an estimate of the molar concentration of enzyme used in assay.

assay format given that the apparent IC_{50} of 2.6 nM was close to the actual molar concentration of enzyme. However, in the [^{3}H]-anandamide assay, the membrane protein concentration used was only 1 μg/mL, which would be equivalent to 0.1 nM given the enzyme titration result. The IC_{50} of 2 nM determined using this assay was therefore unlikely an underestimate due to enzyme titration.

Inhibition of rhFAAH by 1 Is Time-Dependent. The apparent noncompetitive inhibition, the observed failure for rhFAAH activity to recover from preincubation and dilution, and kinetic titration of rhFAAH by **1** would be consistent with the compound being a covalent, irreversible inhibitor of rhFAAH. However, according to Wang et al.,[47] inhibition of FAAH by **1** did not appear to be time-dependent, suggesting a reversible mechanism. Given this potential discrepancy, time-dependent inhibition kinetic experiments were performed with rhFAAH and **1**. As shown in Figure 5A, progress curves of rhFAAH obtained using the D-AMC assay method were linear with time in the absence of inhibitor but curved in the presence of URB597, indicating time-dependent inhibition of rhFAAH by the compound, which is consistent with the nature of the compound acting as a covalent, irreversible inhibitor of FAAH.[35] Analysis of data according to eq 3 assuming the reaction being apparently irreversible ($v_s = 0$) provided estimates of k_{obsd}, the observed inhibition rate constant, and v_i, the initial velocity of rhFAAH at $t = 0$. Reanalysis of k_{obsd} according to eq 4 assuming the apparent irreversibility ($k_4 = 0$) (Figure 5B) yielded estimates of the inhibition rate constant k_3 (0.029 ± 0.001 min^{-1}, Table 2) and the $K_{i(1)}$ for the initial binding of URB597 to rhFAAH (2.0 ± 0.3 μM, Table 2). A K_i value of 3.5 ± 0.6 μM (Table 2) was also obtained through reanalysis of v_i according to eq 5 (Figure 5C). These data indicate that URB597 is a relatively poor binder of rhFAAH for the first initial binding step, consistent with previous findings,[53] and its high overall potency as documented in the literature is mainly derived from the subsequent covalent modification of the enzyme. The progress curves obtained with **1** were also indicative of time-dependent inhibition of rhFAAH by this inhibitor (Figure 6A).

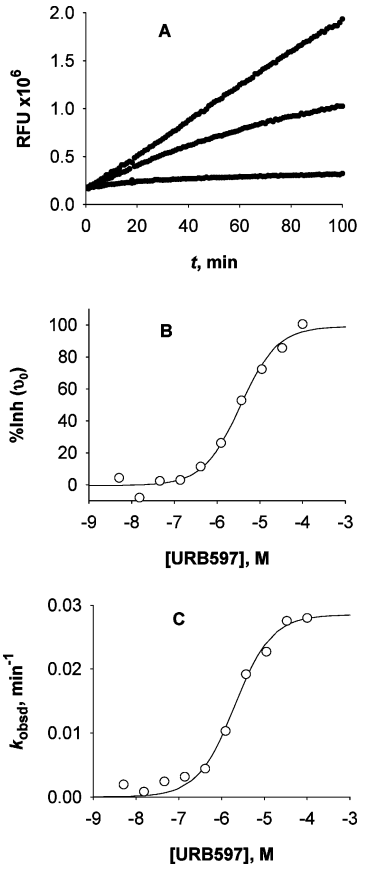

Figure 5. Time-dependent inhibition of rhFAAH by URB597. Time-dependent inhibition kinetics with URB597 were determined by progress curves analysis at pH 8.0 and 22 °C using the D-AMC assay. (A) Enzyme progress curves were obtained at 12 different inhibitor concentrations, and only curves with inhibitor concentrations of 0 (the top curve), 1.2 (the middle curve), and 100 μM (the bottom curve) are shown for clarity. Data were fit to eq 3 (assuming $v_s = 0$) to determine initial rates at $t = 0$ (v_i) and observed inhibition rate constants (k_{obsd}). (B) Percent inhibition (%Inh) as calculated based on v_i was plotted against inhibitor concentration to determine IC_{50} for the initial binding step ($IC_{50(t=0)}$) according to eq 2. (C) Values of k_{obsd} were analyzed using eq 4 (assuming $k_4 = 0$) to calculate the inhibition rate constant k_3 and provide an estimate of $IC_{50(t=0)}$ as well.

Subsequent reanalyses of k_{obsd} (Figure 6B) and v_0 (Figure 6C) according to eqs 4 and 5 yielded respectively a K_i of 7.7 ± 3.4 and 8.4 ± 6.4 nM (Table 2) for the initial inhibitor binding step, values that were, however, quite close to its apparent overall potency (2.6 ± 0.6 nM, Table 1).

The reason for the discrepancy in time-dependent inhibition of rhFAAH by **1** in the current study and that reported by Wang et al.[47] is not clear. In Wang et al.,[47] time dependence of inhibition was assessed by measuring IC_{50} over time, a procedure that may not be as sensitive as progress curves analysis for time-dependent inhibitors for which the time-dependent events improve potency by a relatively small margin as in the case of **1**. Given the fact that covalent and irreversible inhibition in general is time-dependent, the apparent behavior of time dependence observed in our current investigation would seem to be consistent with, but in itself would not necessarily prove, irreversible inhibition.

dx.doi.org/10.1021/bi200552p | Biochemistry 2011, 50, 6867–6878

Table 2. Summary of Time-Dependent Inhibition Properties of URB597 and Benzothiazole Analogue 1[a]

		K_i, μM		
compd	k_3, min^{-1}	from v_i	from k_{obsd}	geomean
URB597	0.029 ± 0.001	3.5 ± 0.6	2.0 ± 0.3	2.7 ± 0.4
1	0.018 ± 0.002	0.0077 ± 0.0034	0.0084 ± 0.0064	0.0080 ± 0.0047

[a]Nonlinear squares analysis of data from progress curves using the D-AMC assay to eq 3 assuming $v_s = 0$ was performed to obtain estimates of k_{obsd}, the observed rate constant for inhibition, and v_i, the initial velocity at $t = 0$, at various inhibitor concentrations. Subsequently, analysis of v_i and k_{obsd} according to eq 4 (assuming $k_4 = 0$) and eq 5 yielded estimates for the values for the initial inhibitor binding step and the inhibition rate constant k_3 for the step following initial binding of inhibitor.

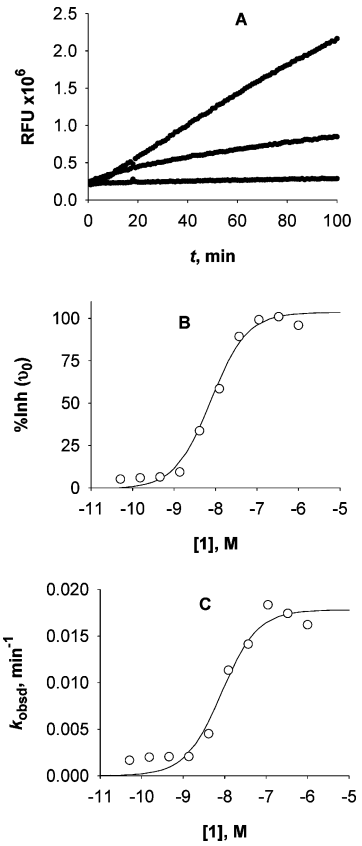

Figure 6. Time-dependent inhibition of rhFAAH by the benzothiazole analogue **1**. Time-dependent inhibition kinetics with **1** were determined by progress curves analysis at pH 8.0 and 22 °C using the D-AMC assay. (A) Enzyme progress curves were obtained at 12 different inhibitor concentrations, and only curves with inhibitor concentrations of 0 (the top curve), 1.2 (the middle curve), and 100 μM (the bottom curve) are shown for clarity. Data were fit to eq 3 (assuming $v_s = 0$) to determine initial rates at $t = 0$ (v_i) and observed inhibition rate constants (k_{obsd}). (B) Percent inhibition (%Inh) as calculated based on v_i was plotted against inhibitor concentration to determine IC_{50} for the initial binding step ($IC_{50(t=0)}$) according to eq 2. (C) Values of k_{obsd} were analyzed using eq 4 (assuming $k_4 = 0$) to calculate the inhibition rate constant k_3 and provide an estimate of $IC_{50(t=0)}$ as well.

Liquid Chromatography Mass Spectrometry Demonstrates Full Recovery of 1 and Fails To Identify Any Cleavage Product or Covalent Adduct from the Enzyme and 1 Incubation Mixture. Membranes of rhFAAH at 3.5 mg/mL were incubated with 1 μM inhibitor overnight and then subjected to liquid chromatography mass spectrometric analysis. When the rhFAAH membranes were incubated with the irreversible carbamate URB597, ~60% of the parent compound was recovered (Figure 7). According to the estimate

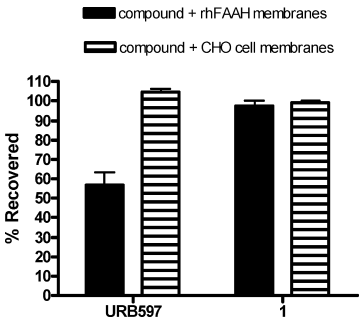

Figure 7. Percent of recovery of the benzothiazole analogue **1** and URB597 from preincubation with rhFAAH as measured by mass spectrometry. Membranes of rhFAAH (3.5 mg/mL) were incubated with inhibitor (1 μM) pH 8.0, at 22 °C overnight and then subjected to liquid chromatography mass spectrometric analysis. After denaturing of the incubation mixture, ~60% of URB597 was recovered, corresponding to a loss of ~0.4 μM inhibitor due to a close to stoichiometric covalent binding of inhibitor to enzyme since 35 mg/mL membranes in the incubation mixture was estimated to contain ~0.35 μM rhFAAH according to enzyme titration. Recovery of **1** was close to 100%, suggesting that it was not covalently bound to enzyme.

(1 μg/mL ≈ 0.1 nM) of the molar concentration of enzyme in the incubation mixture by enzyme titration experiments as described above, of the 1 μM URB597 used in the incubation mixture, 0.35 μM would have been bound to rhFAAH. Therefore, the ~60% recovery of URB597 from the enzyme and inhibitor incubation mixture was almost fully accounted for by assuming a stoichiometric, covalent binding of the inhibitor to enzyme. Subsequent analysis of the denatured supernatant through LC/MS/MS also confirmed formation of the expected carbamate cleavage product as reported previously[35] (data not shown). When the rhFAAH membranes were incubated with **1**, however, virtually all parent compound was recovered from denatured enzyme–inhibitor complex (Figure 7). Further analysis of the denatured supernatant did not identify products that would derive from cleavage of **1** if it had acted as a covalent irreversible inhibitor with cleavage at the amide or sulfonamide bond (data not shown).

Mass spectrometric procedures were also performed to determine if a covalent adduct or intermediate might have formed in the enzyme and inhibitor incubation mixture. In this case, purified humanized rat FAAH (h/rFAAH) was incubated with inhibitor for 1 h before the incubation mixture was subjected to mass spectrometric analyses. When URB597 was used in this procedure, a molecular species with a mass unit of 61774 Da was identified (Figure 8B). That was a gain of 126 mass units compared to the apparent mass of h/rFAAH, an observation fully consistent with reported results where UBR597 carbamylates the enzyme.[35] If **1** had acted similarly, one would expect a molecular weight gain of either 259 (cleavage

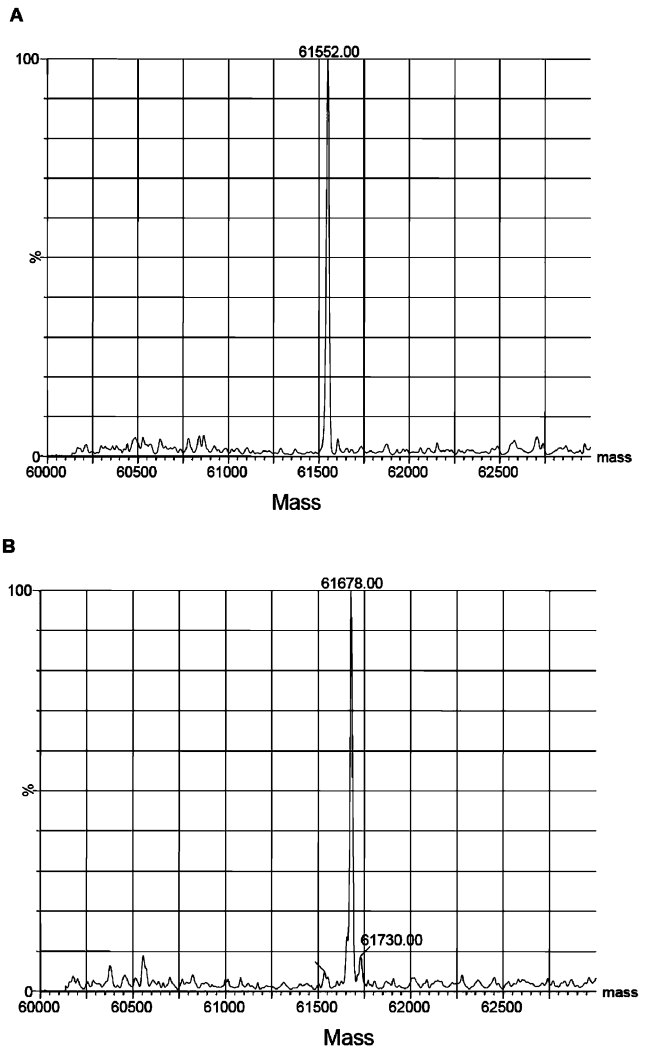

Figure 8. Data from electrospray ionization mass spectroscopic analysis of purified recombinant h/rFAAH incubated with the benzothiazole analogue **1** and URB597. Purified h/rFAAH was incubated at pH 8.0 and 22 °C with **1** for 1 h, and the mixture was denatured and subjected to electrospray ionization mass spectrometry (ESI-MS) analysis. This ESI-MS experiment yielded a peak with a mass of 61552 Da (A), a value within the normally observed variation between 61548 and 61552 Da for h/rFAAH. Preincubation with URB597 yielded a modified enzyme with a mass increase of 126 Da (B), consistent with formation of a covalent adduct derived from cleavage of URB597.

at the amide bond) or 148 (cleavage at the sulfonamide bond) mass units. However, none of these species were visible in the mass spectrometric analyses, and only a species (61552 Da) consistent with the apoenzyme was visible (Figure 8A). These data, although in themselves do not necessarily rule out covalent adduct formation during preincubation with enzyme and subsequent adduct disintegration during mass spectrometry analysis, are consistent with the conclusion of noncovalent inhibition derived from the observations of no cleavage product formation and full recovery of the parent compound from enzyme–inhibitor incubation mixtures.

Benzothiazole Analogue 1 Dissociates Slowly from Enzyme–Inhibitor Complex. Now that covalent irreversible inhibition of rhFAAH by **1** had been ruled out by the mass spectrometric analyses, the only conceivable interpretation of the apparent irreversible kinetics in the D-AMC assay with **1** observed at the beginning of this investigation would seem to be the result of a very slow dissociation rate, too slow to show characteristics of reversible kinetics during the 4 h assay time of the D-AMC assay. To evaluate this possibility, rhFAAH and **1** were preincubated for 1 h and then dialyzed for 18 h. As shown in Figure 9, the enzyme activity recovered, albeit very slowly,

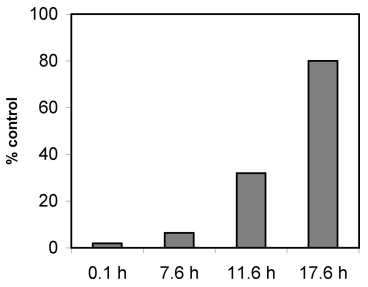

Figure 9. Recovery of rhFAAH activity by dialysis of the enzyme–inhibitor complex formed from incubation of rhFAAH and the benzothiazole analogue **1**. Membranes of rhFAAH at 35 μg/mL (final concentration in assay) were incubated in the presence or absence of 1 μM of **1** at pH 8.0 and 22 °C for 1 h. The mixture was then diluted and centrifuged to remove excess inhibitor. The pellet was resuspended and the suspension placed in a dialysis cassette. This dialysis cassette was placed in 4 L of assay buffer that had been pre-equilibrated at 4 °C. An aliquot was withdrawn using a syringe at different times to determine FAAH activity using the D-AMC assay over a period of 18 h.

demonstrating that the inhibition of rhFAAH by **1** was indeed kinetically reversible.

Do Benzothiazoles Represent a New Class of FAAH Inhibitors That Are Transition-State Analogues?

Through computer modeling comparing hypothetical binding modes of **1** and the covalently attached methoxy arachidonyl phosphonate in the rFAAH crystal structure,[51] Wang et al. postulated that the sulfone in **1** could mimic the tetrahedral hemiacetal at the covalent attachment site for α-ketone heterocycles without forming a covalent bond with the catalytic serine,[47] thereby acting in essence as a transition-state analogue of the enzyme. Since enzymes catalyze biochemical reactions by stabilizing transition state, this hypothesis of **1** acting as a transition state analogue would help explain why this noncovalent, reversible inhibitor inhibits FAAH with such a high potency.

According to known crystal structures,[48,51] the FAAH active site contains a long acyl chain binding pocket that is part of a longer substrate entry tunnel and a shorter, polar amine product exit tunnel oriented at about an 80° angle from the acyl chain binding pocket, with the catalytic triad located at the corner connecting the two tunnels.[51] The catalytic site is also the location of two amide nitrogens from Ile-238 and Gly-239 that are seen hydrogen-bonded to the phosphono oxygen of the covalently attached methoxy arachidonyl phosphonate in the rFAAH crystal structure[51] or to the carbonyl oxygen of the covalently attached arylurea PF-750 in the h/rFAAH crystal structure.[48] This backbone hydrogen-bonding contribution was also observed from Monte Carlo simulations for α-keto oxazole derivatives covalently bound to the enzyme.[30] Such a hydrogen-bonding interaction suggests that these two amide nitrogens function as an "anion hole" that helps neutralize the evolving hemiacetal oxyanion during catalysis, thereby stabilizing the transition state.

Molecular modeling to dock **1** into the crystal structure of h/rFAAH was performed using an induced fit procedure to

dx.doi.org/10.1021/bi200552p | Biochemistry 2011, 50, 6867–6878

provide additional insights into the structural features of **1** binding at the active site. This docking procedure allows a limited degree of movements for the enzyme, thereby providing possibly a more accurate presentation of the docked complex than a simple, one-step docking method. Figure 10A shows the

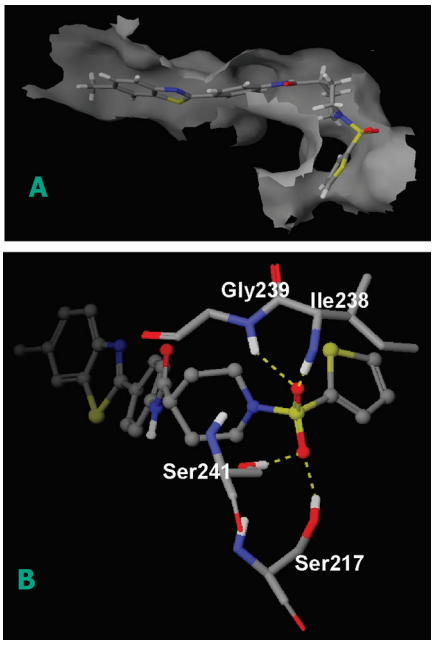

Figure 10. Molecular modeling by docking of the benzothiazole analogue **1** into the h/rFAAH active site. The benzothiazole analogue **1** was docked into the h/rFAAH active site through an induced fit docking procedure, producing a structure where both the catalytic serines, Ser-241 and Ser-217, form a hydrogen bond with a sulfone oxygen while two backbone residues Ile-238 and Gly-239, postulated to act as an "anion hole", provide a hydrogen bond to the other sulfone oxygen.

overall topology of the docked **1** structure, with the thiophene moiety occupying the product exit tunnel and the portion containing the benzothiazole group traversing much of the acyl chain binding pocket. In this docked structure, both the catalytic serines, Ser-241 and Ser-217, form hydrogen bonds with one sulfone oxygen while each of the postulated "anion hole" nitrogens of Ile-238 and Gly-239 provide hydrogen bonds to the other sulfone oxygen (Figure 10B). Such a strong hydrogen-bonding network engaging the sulfonamide group is analogous to transition state stabilization during the FAAH catalysis and may explain, at least in part, why **1**, a reversible noncovalent inhibitor, inhibits rhFAAH with great potency.

DISCUSSION

A primary objective of the current investigation was to elucidate the mechanism of inhibition of FAAH by the benzothiazole analogue **1**, a potent, low nM inhibitor with an intriguing structure containing both an amide and a sulfonamide moiety.[47] A key question to address was whether this potent molecule inhibits FAAH irreversibly and/or by covalent interactions.

Two pieces of data were presented by Wang et al.[47] to suggest that the inhibition of FAAH by benzothiazole analogues may not be covalent in nature. The first was based on the observation that the inhibition of FAAH did not appear to be time dependent. Although time dependence is often associated with covalent inhibition, the lack of time dependence in itself does not necessarily rule out covalent inhibition. The second argument was derived from the observation that converting the amide carbonyl to a methylene group did not perturb the potency of the compound, suggesting that this inhibitor employs a mechanism different from the mechanism for activated ketones where formation of a hemiacetal covalent adduct with the catalytic serine residue is the main force driving the potency of such inhibitors. However, the potency of the compound appeared to depend greatly upon the presence of the sulfonyl group of **1**, leaving open the possibility of covalent interactions between FAAH and **1** through this sulfonamide moiety. Although covalent modification through sulfonamides is rare, it is theoretically possible and would not be totally surprising in this case given that molecules chemically stable under normal conditions, such as arylureas, can act as covalent inhibitors of this particular enzyme. The answer to this question is important for drug discovery efforts in that should the inhibition be indeed reversible and noncovalent it would validate efforts pursuing noncovalent reversible drug candidates targeting FAAH, a strategy generally favored in conventional drug discovery processes.

In the current investigation, the failure to observe the formation of covalent enzyme−inhibitor adduct (Figure 8) or putative cleavage product (Figure 7) using electrospray MS techniques provided strong physical evidence against covalent inhibition of FAAH by **1**. Recovery of enzyme activity of FAAH preincubated with **1** through a dialysis procedure demonstrated unequivocally that the inhibition of FAAH by **1** is kinetically reversible. Although the compound displayed noncompetitive, time-dependent, and apparently irreversible inhibition from a preincubation and dilution procedure, all these characteristics of seemly covalent and irreversible inhibition could be explained as arising from the nonequilibrium conditions as a result of the assay time (4 h) being shorter than the residence time of the inhibitor (>11.6 h, Figure 9).

While most known FAAH inhibitors are covalent and irreversible, a number of reversible FAAH inhibitors have been reported recently,[52,54] although it is not known whether they act via a covalent or noncovalent mechanism. Nevertheless, **1**, possessing a single digit nM potency, is by far the most potent noncovalent and reversible inhibitor of FAAH described to date. This high potency may be related to the nature of the interaction of **1** adopting a transition state with the residues involved in the catalytic "anion hole" as suggested through a computational analysis of **1** docked into the active site of FAAH (Figure 10). The notion of **1** acting as a transition state analogue is a new concept for the FAAH inhibition and, if proven to be true, would open the door to developing novel FAAH inhibitors by targeting the catalytic hydrogen-bonding network involving not only the catalytic serines but also the "anion hole" amide nitrogens.

It is interesting that **1**, noncovalent and reversible without being exceedingly potent ($IC_{50} \sim 2$ nM), displays a very long residence time ($t_{1/2} > 11.6$ h). For a reversible inhibitor to display such a long residence time, it generally requires the inhibitor to possess a high thermodynamic potency if the long residence time is purely potency driven. This is understood theoretically assuming a one-step binding mechanism where the association rate constant k_{on} is diffusion-controlled. For example, an inhibitor with a $t_{1/2} = 10$ h or the dissociation rate constant $k_{off} = 0.000019\ s^{-1}$ would require the K_d to be as low as 1.9 pM, assuming a k_{on} of $10^7\ M^{-1}\ s^{-1}$. Several drugs

dx.doi.org/10.1021/bi200552p | *Biochemistry* 2011, 50, 6867–6878

known to have very long residence times fall in this category.[55−57] The same argument also applies to inhibitors with a two-step binding mechanism where the second step is fast and not rate-limiting (see below). Compound **1** clearly represents a different class of long residence time inhibitors,[55−57] those having a two-step mechanism (eq 6):

$$\mathrm{E} + \mathrm{I} \underset{k_2}{\overset{k_1}{\rightleftharpoons}} \mathrm{EI} \underset{k_4}{\overset{k_3}{\rightleftharpoons}} \mathrm{EI}^* \tag{6}$$

with the second step being relatively slow and rate-limiting (Figure 6).

For such an inhibition mechanism, the overall potency $K_{i(overall)}$ of the compound is given by eq 7:

$$K_{i(overall)} = \frac{[E][I]}{[EI] + [EI]} = \frac{K_i}{1 + \frac{1}{K_2}} \tag{7}$$

where $K_2 = k_4/k_3$. The initial inhibition constant K_i (k_2/k_1) of 8 nM and the rate constant k_3 of 0.018 min^{-1} (Table 2) for compound **1** were determined assuming the second step was irreversible, which is a reasonable approximation given the observed long residence time (Figure 9) . The $t_{1/2}$ for the overall dissociation was ~11.6 h (Figure 9), which would translate into a k_{off} value of ~0.0010 min^{-1}. For a two-step process, the k_{off} is given by eq 8:[56]

$$k_{off} = \frac{k_2 k_4}{k_2 + k_3 + k_4} \tag{8}$$

Assuming a relatively small k_3 and k_4 compared to k_2, eq 8 is reduced to $k_{off} \approx k_4 \sim 0.0010$ min^{-1}. Thus, K_2 may be calculated using k_3 (0.018 min^{-1}) and the estimated k_4 (~0.0010 min^{-1}) to be ~0.056. With this K_2 value and the determined K_i of 8 nM (Table 2), the $K_{i(overall)}$ can be estimated using eq 7 to be ~0.43 nM. This calculated value is ~5-fold less than the IC_{50} values determined using either the D-AMC assay (2.6 nM) or the [^{3}H]-anandamide assay (2 nM). This discrepancy is likely a result of enzyme titration in the D-AMC assay as the effective enzyme concentration in this assay was estimated to be 3.5 nM (see in Results section), a value close to the apparent IC_{50}, and the relatively short assay time (30 min) in the [^{3}H]-anandamide assay that was comparable to the time scale for inhibitor association ($t_{1/2}$ = 39 min as calculated from the k_3 value, Table 2).

While this calculated $K_{i(overall)}$ value of 0.43 nM is by far the most potent among known reversible, noncovalent FAAH inhibitors, it is probably 2 orders of magnitude weaker than what might be necessary for a compound to derive a $t_{1/2}$ > 10 h purely from thermodynamic potency as discussed above. Clearly, in the inhibition of FAHH by **1**, the observed long residence time is related to the relatively slow second step, which corresponds to a kinetic barrier that is higher than that of the diffusion-controlled association of inhibitor and enzyme.

The contribution from increased kinetic energy barriers to the observed residence time may be illustrated by an analysis of the energetics of the binding reaction for a two-step mechanism as depicted in Figure 11. Assuming a diffusion-controlled association of enzyme and inhibitor, if the kinetic energy barrier for the second step (transition state 2 (TS2)) is insignificant compared to the kinetic barrier to the first step (TS1) ($k_3 \gg k_2$), the

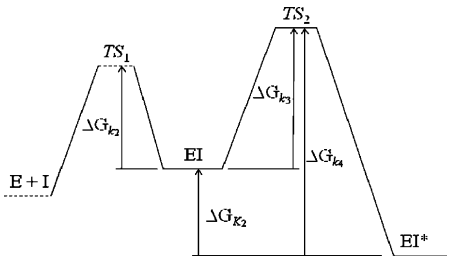

Figure 11. Energy diagram of two-step binding reaction. The energy states are indicated for the free enzyme and inhibitor (E + I), the initial enzyme−inhibitor complex EI, and the final enzyme−inhibitor complex EI*. The free energies ΔG_{k_2}, ΔG_{k_3}, and ΔG_{k_4} represent kinetic energy barriers for dissociation of EI, formation of EI*, and dissociation of EI*, respectively. The free energy ΔG_{K_2} represents the thermodynamic energy of the equilibrium between EI and EI*. TS_1 and TS_2 represent respectively the transition state for the initial binding and the transition state for the conversion of EI to EI*.

effective kinetic energy barrier to the overall dissociation ($\Delta G_{k_{off}}$) would be approximated by the sum of the kinetic energy barrier to dissociation of EI (ΔG_{k_2}) and the thermodynamic energy required for the formation of EI* from EI (ΔG_{K_2}). Accordingly, the effective dissociation rate constant (eq 8) would be approximated by eq 9 given a large k_3 compared to k_2 and k_4:

$$k_{off} = k_2 \frac{k_4}{k_3} = k_2 K_2 \tag{9}$$

In energy terms, eq 9 may be expressed as

$$\Delta G_{k_{off}} = -RT \ln k_2 - RT \ln K_2 = \Delta G_{k_2} + \Delta G_{K_2} \tag{10}$$

which is the sum of the kinetic energy barrier to the dissociation of EI and the thermodynamic energy for the formation of EI* from EI. In this case, a very high potency (i.e., in the pM range) is generally required for the inhibitor to display a very long residence time just as inhibitors of diffusion-controlled one-step binding. On the other hand, if the second step is slow and rate-limiting as in the inhibition of FAAH by **1**, eq 8 becomes

$$k_{off} = k_4 \tag{11}$$

and the energy barrier to dissociation would then be given by

$$\Delta G_{k_{off}} = -RT \ln k_4 = \Delta G_{k_4} \tag{12}$$

which is the kinetic energy barrier (TS_2) increased over that for the initial binding (TS_1) due to the slow, time-dependent second step. With potency being constant, the slower the second step, the longer the residence time would be. With a rate-limiting and relatively slow second step, compound **1** fits nicely in this class of long residence time inhibitors, displaying a very long residence time ($t_{1/2}$ > 11.6 h) without possessing an exceedingly high thermodynamic potency.

It has been recognized[55,56] that a long drug residence can be achieved by increased kinetic barrier due to time-dependent rate-limiting steps in a multiple-step binding reaction. Our results demonstrate that only a moderately slow time-dependent binding step ($t_{1/2}$ = 38 min calculated using k_3 = 0.018 min, Table 2) is sufficient for an inhibitor such as **1** to display a very long residence time ($t_{1/2}$ = 11.6 h) even though their thermodynamic potency is not exceedingly high. For a

dx.doi.org/10.1021/bi200552p | Biochemistry 2011, 50, 6867−6878

long residence time inhibitor to show efficacy *in vivo*, the lifetime of the drug in circulation (e.g., 5 h) needs to be longer than the time for inhibitor binding to the target (38 min for **1**), but can be much shorter than the residence time (11.6 h for **1**). Thus, the duration of pharmacological effect can greatly exceed the lifetime predicted from circulating drug levels. The extended duration of action *in vivo* means that a reduced dosing schedule can achieve the desired therapeutic effect, which might also provide a more favorable safety profile if off-target adverse effects are a concern. Compound **1** displays a unique mechanistic profile as a long residence time FAAH inhibitor that does not covalently modify the active site serine. The structural features that underpin its interaction with FAAH offer new avenues into the development of compounds with potential for long-lasting modulation of endocannabinoid tone in disease states.

AUTHOR INFORMATION

Corresponding Author

*Tel: 610-917-6713. Fax: 610-917-6786. E-mail: gaochao.x.tian@gsk.com.

Present Addresses

[#]Biological Reagents and Assay Development, Platform Technology and Science, GlaxoSmithKline, 1250 South Collegeville Road, Collegeville, PA 19426.

[&]Bioanalytical Sciences, MedImmune, One MedImmune Way, Gaithersburg, MD 20878.

ACKNOWLEDGMENTS

We are grateful for Luc Meury for preparation of rhFAAH membranes, Russ Mauger for synthesis of D-AMC, and Phil Edwards and Jeff Varnes for discussion and insight regarding mechanistic properties of FAAH inhibitors.

ABREVIATIONS

BSA, bovine serum albumin; D-AMC, decanoyl 7-amino-4-methylcoumarin; CB1, cannabinoid receptor 1; DDM, *n*-dodecyl-*β*-D-maltopyranoside; DMSO, dimethyl sulfoxide; FAAH, fatty acid amide hydrolase; rhFAAH, recombinant human FAAH; rFAAH, rat FAAH; h/rFAAH, humanized rFAAH; CHO, Chinese hamster ovary.

REFERENCES

(1) Cravatt, B. F., Giang, D. K., Mayfield, S. P., Boger, D. L., Lerner, R. A., and Gilula, N. B. (1996) Molecular characterization of an enzyme that degrades neuromodulatory fatty-acid amides. *Nature 384*, 83−87.

(2) Chebrou, H., Bigey, F., Arnaud, A., and Galzy, P. (1996) Study of the amidase signature group. *Biochim. Biophys. Acta 1298*, 285−293.

(3) McKinney, M. K., and Cravatt, B. F. (2005) Structure and function of fatty acid amide hydrolase. *Annu. Rev. Biochem. 74*, 411−432.

(4) Devane, W. A., Hanus, L., Breuer, A., Pertwee, R. G., Stevenson, L. A., Griffin, G., Gibson, D., Mandelbaum, A., Etinger, A., and Mechoulam, R. (1992) Isolation and structure of a brain constituent that binds to the cannabinoid receptor. *Science 258*, 1946−1949.

(5) Cravatt, B. F., Demarest, K., Patricelli, M. P., Bracey, M. H., Giang, D. K., Martin, B. R., and Lichtman, A. H. (2001) Supersensitivity to anandamide and enhanced endogenous cannabinoid signaling in mice lacking fatty acid amide hydrolase. *Proc. Natl. Acad. Sci. U. S. A. 98*, 9371−0376.

(6) Kathuria, S., Gaetani, S., Fegley, D., Valino, F., Duranti, A., Tontini, A., Mor, M., Tarzia, G., La Rana, G., Calignano, A., Giustino, A., Tatolli, M., Palmery, M., Cuomo, V., and Piomelli, D. (2003) Modulation of anxiety through blockade of anandamide hydrolysis. *Nature Med. 9*, 76−81.

(7) Lichtman, A. H., Shelton, C. C., Advani, T., and Cravatt, B. F. (2004) Mice lacking fatty acid amide hydrolase exhibit a cannabinoid receptor-mediated phenotypic hypoalgesia. *Pain 109*, 319−327.

(8) Hohmann, A. G., Suplita, R. L., Bolton, N. M., Neely, M. H., Fegley, D., Mangieri, R., Krey, J. F., Walker, J. M., Holmes, P. V., Crystal, J. D., Duranti, A., Tontini, A., Mor, M., Tarzia, G., and Piomelli, D. (2005) An endocannabinoid mechanism for stress-induced analgesia. *Nature 435*, 1108−1112.

(9) Jayamanne, A., Greenwood, R., Mitchell, V. A., Aslan, S., Piomelli, D., and Vaughan, C. W. (2006) Actions of the fatty acid amide hydrolase inhibitor URB597 in neuropathic and inflammatory chronic pain models. *Br. J. Pharmacol. 147*, 281−288.

(10) Chang, L., Luo, L., Palmer, J. A., Sutton, S., Wilson, S. J., Barbier, A. J., Breitenbucher, J. G., Chaplan, S. R., and Webb, M. (2006) Inhibition of fatty acid amide hydrolase produces analgesia by multiple mechanisms. *Br. J. Pharmacol. 148*, 102−113.

(11) Russo, R., LoVerme, J., La Rana, G., Compton, T., Parrot, J., Duranti, A., Tontini, A., Mor, M., Tarzia, G., Calignano, A., and Piomelli, D. (2007) The fatty acid amide hydrolase inhibitor URB597 (cyclohexylcarbomic acid 3′-carbomoyl-biphenyl-3-yl ester) reduces neuropathic pain after oral administration in mice. *J. Pharmacol. Exp. Ther. 322*, 236−242.

(12) Gobbi, G., Bambico, F. R., Mangieri, R., Bortolato, M., Campplongo, P., Solinas, M., Cassano, T., Morgese, M. G., Debbonnel, G., Duranti, A., Tontini, A., Tarzia, G., Mor, M., Trezza, V., Goldberg, S. R., Cuomo, V., and Piomelli, D. (2005) Antidepressant-like activity and modulation of brain monoaminergic transmission by blockade of anandamide hydrolysis. *Proc. Natl. Acad. Sci. U. S. A. 102*, 18620−18625.

(13) Naiu, P. S., Varvel, S. A., Ahn, K., Cravatt, B. F., Martin, B. R., and Lichtman, A. H. (2006) Evaluation of fatty acid amide hydrolase inhibition in murine models of emotionality. *Psychopharmacology 192*, 61−70.

(14) Huitron-Resendiz, S., Sanchez-Alavez, M., Wills, D. N., Cravatt, B. F., and Henriksen, S. J. (2004) Characterization of sleep-wake patterns in mice lacking fatty acid amide hydrolase. *Sleep 27*, 857−865.

(15) Varvel, S.A., Wise, L. E., Niyuhire, F., Cravatt, B. F., and Lichtman, A. H. (2007) Inhibition of fatty acid amide hydrolase accelerates acquisition and extinction rates in a spatial memory task. *Neuropsychopharmacology 32*, 1032−1041.

(16) Massa, F., Marsicano, G., Hermann, H., Cannich, A., Monory, K., Cravatt, B. F., Ferri, G.-L., Sibaev, A., Stoor, M., and Lutz, B. (2004) The endogenous cannabinoid system protectsagainst colonic inflammation. *J. Clin. Invest. 113*, 1202−1209.

(17) Cravatt, B. F., Saghatelian, A., Hawkins, E. G., Clement, A. B., Bracey, M. H., and Lichtman, A. H. (2004) Functional dissociation of the central and peripheral fatty acid amide signaling systems. *Proc. Natl. Acad. Sci. U. S. A. 101*, 10821−10826.

(18) Holt, S., Comelli, F., Costa, B., and Fowler, C. J. (2005) Inhibitors of fatty acid amide hydrolase reduce carrageenan-induced hind paw inflammation in pentobarbital-treated mice: comparison with indomethacin and possible involvement of cannabinoid receptors. *Br. J. Pharmacol. 146*, 467−476.

(19) Karsak, M., Gaffal, E., Date, R., Wang-Eckhardt, L., Rehnelt, J., Petrosino, S., Starowicz, K., Steuder, R., Schlicker, E., Cravatt, B. F., Meucholam, R., Buettner, R., Werner, S., Di Marzo, V., Tuting, T., and Zimmer, A. (2007) Attenuation of allergic contact dermatitis through the endocannabinoid system. *Science 316*, 1494−1497.

(20) Lambert, D. M., and Fowler, C. J. (2005) The endocannabinoid system: drug targets, lead compounds, and potential therapeutic applications. *J. Med. Chem. 48*, 5059−5087.

(21) Seierstad, M., and Breitenbucher, J. G. (2008) Discovery and development of fatty acid amide hydrolase (FAAH) inhibitors. *J. Med. Chem. 51*, 7327−7343.

(22) Deutsch, D. G., and Chin, S, A. (1993) Enzymatic synthesis and degradation of anandamide, a cannabinoid receptor agonist. *Biochem. Pharmacol. 46*, 791−796.

(23) Deutsch, D. G., Lin, S., Hill, W. A. G., Morse, K. L., Salehani, D., Arreaza, G., Omeir, R. L., and Makriyannis, A. (1997) Fatty acid sulfonylfluorides inhibit anandamide metabolism and bind to the cannabinoid receptor. *Biochem. Biophys. Res. Commun. 231*, 217−221.

(24) Patricelli, M. P., Lovato, M. A., and Cravatt, B. F. (1999) Chemical and mutagenic investigations of fatty acid amide hydrolase: evidence for a family of serine hydrolases with distinct catalytic properties. *Biochemistry 38*, 9804−9812.

(25) Deutsch, D. G., Omeir, R., Arreaza, G., Salehani, D., Prestwich, G. D., Huang, Z., and Howlett, A. (1997) Methyl arachidonyl fluorophosphonate: a potent irreversible anandamide amidase. *Biochem. Pharmacol. 53*, 255−260.

(26) De Petrocellis, L., Melck, D., Ueda, N., Maurelli, S., Kurahashi, Y., Yamamoto, S., Marino, G., and Di Marzo, V. (1997) Novel inhibitors of brain, neuronal, and basophilic anandamide amidohydrolase. *Biochem. Biophys. Res. Commun. 231*, 82−88.

(27) Koutek, B., Prestwich, G. D., Howlett, A. C., Chin, S. A., Salehani, D., Akhavan, N., and Deutsch, D. G. (1994) Inhibitors of arachidonoyl ethanolamide hydrolysis. *J. Biol. Chem. 269*, 22937−22940.

(28) Patterson, J. E., Ollman, I. R., Cravatt, B. F., Boger, D. L., Wong, C. H., and Lerner, R. A. (1996) Inhibition of oleamide hydrolase catalyzed hydrolysis of the endogenous sleep-inducing lipid cis-9-octadecenamide. *J. Am. Chem. Soc. 118*, 5938−5945.

(29) Boger, D. L., Sato, H., Lerner, A. E., Austin, B. J., Patterson, J. E., Patricelli, M. P., and Cravatt, B. F. (1999) Trifluoromethyl ketone inhibitors of fatty acid amide hydrolase: a probe of structural and conformational features contributing to inhibition. *Bioorg. Med. Chem. Lett. 9*, 265−270.

(30) Boger, D. L., Miyauchi, H., Du, W., Hardouin, C., Fecik, R. A., Cheng, H., Hwang, I., Hedrick, M. P., Leung, D., Acevedo, O., Guimaraes, C. R. W., Jorgensen, W. L., and Cravatt, B. F. (2005) Discovery of a potent, selective, and efficacious class of reversible a-ketoheterocycle inhibitors of fatty acid amide hydrolase effective as analgesics. *J. Med. Chem. 48*, 1849−1856.

(31) Romero, A., Du, W., Hwang, I., Rayl, T. J. F., Kimball, S., Leung, D., Hoover, H. S., Apodaca, R. L., Breitenbucher, J. G., Cravatt, B. F., and Boger, D. L. (2007) Potent and selective alpha-ketoheterocycle-based inhibitors of the anandamide and oleamide catabolizing enzyme: fatty acid amide hydrolase. *J. Med. Chem. 50*, 1058−1068.

(32) Maryanoff, B. E., and Costanzo, M. J. (2008) Inhibitors of proteases and amide hydrolases that employ an alpha-ketoheterocycle as a key enabling functionality. *Bioorg. Med. Chem. 16*, 1562−1595.

(33) Tarzia, G., Duranti, A., Tontini, A., Piersanti, G., Mor, M., Rivara, S., Plazzi, P. V., Park, C., Kathuria, S., and Piomelli, D. (2003) Design, synthesis, and structure-activity relationships of alkylcarbamic acid aryl esters, a new class of fatty acid amide hydrolase inhibitors. *J. Med. Chem. 46*, 2352−2360.

(34) Mor, M., Rivara, S., Lodola, A., Plazzi, P. V., Tarzia, G., Duranti, A., Tontini, A., Piersanti, G., Kathuria, S., and Piomelli, D. (2004) Cyclohexylcarbamic acid 3′- or 4′-substituted biphenyl-3-yl esters as fatty acid amide hydrolase inhibitors: synthesis, quantitative structure-activity relationships, and molecular modeling studies. *J. Med. Chem. 47*, 4998−5008.

(35) Alexander, J. P., and Cravatt, B. F. (2005) Mechanism of carbamate inactivation of FAAH: implications for the design of covalent inhibitors and in vivo probes of enzymes. *Chem. Biol. 12*, 1179−1187.

(36) Sit, S. Y., Conway, C., Bertekap, R., Xie, K., Bourin, C., Burris, K., and Deng, H. (2007) Novel inhibitors of fatty acid amide hydrolase. *Bioorg. Med. Chem. Lett. 17*, 3287−3291.

(37) Myllymaki, M. J., Saario, S. M., Kataja, A. O., Castillo-Melendez, J. A., Nevalainen, T., Juvonen, R. O., Jarvinen, T., and Koskinen, A. M. P. (2007) Design, synthesis, and in vitro evaluation of carbamate derivatives of 2-benzoxazolyl- and 2-benzothiazolyl-(3-hydroxyphenyl)-methanones as novel fatty acid amide hydrolase. *J. Med. Cem. 50*, 4236−4242.

(38) Allexander, J. P., and Cravatt, B. F. (2006) The putative endocannabinoid transporter blocker LY2183240 is a potent inhibitor of FAAH and several other brain serine hydrolases. *J. Am. Chem. Soc. 128*, 9699−9704.

(39) Ahn, K., Johnson, D. S., Fitzgerald, L. R., Liimatta, M., Arendse, A., Stevenson, T., Lund, E. T., Nugent, R. A., Normanbhoy, T. K., Alexander, J. P., and Cravatt, B. F. (2007) Novel mechanistic class of fatty acid amide hydrolase inhibitors with remarkable selectivity. *Biochemistry 46*, 13019−13030.

(40) Keith, J. M., Apodaca, R., Xiao, W., Seierstad, M., Pattabiraman, K., Wu, J., Webb, M., Karbarz, M., Brown, S., Wilson, S., Scott, B., Tham, C.-S., Luo, L., Palmer, J., Wennerholm, M., Chaplan, S., and Breitenbucher, J. G. (2008) Thiadiazolopiperazinyl ureas as inhibitors of fatty acid amide hydrolase. *Bioorg. Med. Chem. Lett. 18*, 4838−4843.

(41) Johnson, D. S., Stiff, C., Lazerwith, S. E., Kesten, S. R., Lorraine, K. F., Morris, M., Beidler, D., Liimatta, M. B., Smith, S. E., Dudley, D. T., Sadagopan, N., Bhattachar, S. N., Kesten, S. J., Nomanbhoy, T. K., Cravatt, B. F., and Ahn, K. (2011) Discovery of PF-04457845: A highly potent, orally bioavailable, and selective urea FAAH inhibitor. *ACS Med. Chem. Lett. 2*, 91−96.

(42) Holt, S., Nisson, J., Omeir, R., Tiger, G., and Fowler, C. J. (2001) Effects of pH on the inhibition of fatty acid amide hydrolase by ibuprofen. *Br. J. Pharmacol. 133*, 513−520.

(43) Holt, S., Paylor, B., Boldrup, L., Alajakku, K., Vandevoorde, S., Sundstrom, A., Cocco, M. T., Onnis, V., and Fowler, C. J. (2007) Inhibition of fatty acid amide hydrolase, a key endocannabinoid metabolizing enzyme, by analogues of ibuprofen and indomethacin. *Eur. J. Pharmacol. 565*, 26−36.

(44) Bisogno, T., Melck, D., De Petrocellis, L., Bobrov, M. Y., Gretskaya, N. M., Bezuglow, V. V., Sitachitta, N., Gerwick, W. H., and Di Marzo, V. (1998) Arachidonoylserotonin and other novel inhibitors of fatty acid amide hydrolase. *Biochem. Biophys. Res. Commun. 248*, 515−522.

(45) Di Marzo, V., Bisogno, T., De Petrocellis, L., Melck, D., Orlando, P., Wagner, J. A., and Kunos, G. (1999) Biosynthesis and inactivation of the endocannabinoid 2-arachidonoylglycerol in circulating and tumoral macrophages. *Eur. J. Biochem. 264*, 258−267.

(46) Jarrahiam, A., Manna, S., Edgemond, W. S., Campbell, W. B., and Hillhard, C. J. (2000) Structure-activity relationships among *N*-arachidonoylethanolamine (anandamide) head group analogues for the anandamide transporter. *J. Neurochem. 74*, 2597−2606.

(47) Wang, X., Sarris, K., Kage, K., Zhang, D., Brown, S. P., Kolasa, T., Surowy, C., Kouhen, O. F. E., Muchmore, S. W., Brioni, J. D., and Stewart, A. O. (2009) Synthesis and evaluation of benzothiazole-based analogues as novel, potent, and selective fatty acid amide hydrolase inhibitors. *J. Med. Chem. 52*, 170−180.

(48) Mileni, M., Johnson, D. S., Wang, Z., Everdeen, D. S., Liimatta, M., Pabst, B., Bhattacharya, K., Nugent, R. A., Kamtehar, S., Cravatt, B. F., Ahn, K., and Stevens, R. C. (2008) Structure-guided inhibitor design for human FAAH by interspecies active site conversion. *Proc. Natl. Acad. Sci. U. S. A. 105*, 12820−12824.

(49) Kage, K. L., Richardson, P. L., Traphagen, L., Severin, J., Pereda-Lopez, A., Lubben, T., Davis-Taber, R., Vos, M. H., Bartley, D., Walter, K., Harlan, J., Solomon, L., Warrior, U., Holzman, T. F., Faltynek, C., Surowy, C. S., and Scott, V. E. (2007) A high throughput fluorescent assay for measuring the activity of fatty acid amide hydrolase. *J. Neurosci. Met. 161*, 47−54.

(50) Wilson, S. J., Lovenberg, T. W., and Barbier, A. J. (2003) A high-throughput-compatible assay for determining the activity of fatty acid amide hydrolase. *Anal. Biochem. 318*, 270−275.

(51) Bracey, M. H., Hanson, M. A., Masuda, K. R., Stevens, R. C., and Cravatt, B. F. (2002) Structural adaptation in a membrane enzyme that terminates endocannabinoid signaling. *Science 298*, 1793−1796.

(52) Feledziak, M., Michaux, C., Urbach, A., Labar, G., Muccioli, G. G., Lambert, D. M., and Marchand-Brynaert, J. (2009) Beta-lactams derived from a carbapenem chiron are selective inhibitors of human fatty acid amide hydrolase versus human monoacylglycerol lipase. *J. Med. Chem. 52*, 7054−7068.

(53) Ahn, K., Johnson, D. S., Mileni, M., Beidler, D., Long, J. Z., McKinney, M. K., Weerapana, E., Sadagopan, N., Liimatta, M., Smith, S. E., Lazerwith, S., Stiff, C., Kamtekar, S., Bhattacharya, K., Zhang, Y., Swaney, S., Becelaere, K. V., Stevens, R. C., and Cravatt, B. F. (2009) Discovery and characterization of a highly selective FAAH inhibitor that reduces inflammatory pain. *Chem. Biol. 16*, 411−420.

(54) Gattinoni, S., Simone, C. D., Dallavalle, S., Fezza, F., Nannei, R., Battista, N., Minetti, P., Quattrociocchi, G., Caprioli, A., Borsini, F., Cabri, W., Penco, S., Merlini, L., and Maccarrone, M. (2010) A new group of oxime carbamates as reversible inhibitors of fatty acid amide hydrolase. *Bioorg. Med. Chem. Lett. 20*, 4406−4411.

(55) Copeland, R. A., Pompliano, D. L., and Meek, T. D. (2006) Drugtarget residence time and its implications for lead optimization. *Nat. Rev. Drug Discovery 5*, 730−739.

(56) Tummino, P.J., and Copeland, R. A. (2008) Residence time of receptor-ligand complexes and its effect on biological function. *Biochemistry 47*, 5481−5492.

(57) Copeland, R. A. (2005) *Evaluation of Enzyme Inhibitors in Drug Discovery: A Guide for Medicinal Chemists and Pharmacologists*, Wiley, New York.